

# Transformer Synthesis for VHF Converters

Topic Area: 1

## I. INTRODUCTION

The search for reduced size, weight, and cost of power converters has taken many forms. Here we address the synthesis of air-core magnetic structures suitable for use in very high frequency (VHF 30-300 MHz) power converters such as those proposed in [1], [2]. By combining multiple components into a single, planar structure (in this case a two-winding transformer), a reduction in volume and complexity is realized that will help to achieve VHF converter designs with co-packaged energy storage.

In Section II the problem of synthesizing a physical structure that has a desired inductance matrix is discussed. In particular, it addresses efficient means to utilize numerical simulation, which is necessary for most non-trivial air-core structures if skin and proximity effects are important. Section III-A discusses the fabrication of two sets of transformers on printed circuit board (PCB) substrates and compares experimental results to simulated designs. Finally, an isolated  $\Phi_2$  converter is fabricated using a selected transformer. The experimental results are presented in Section III-B.

## II. SYNTHESIS

The general problem addressed in this paper is the question of how to synthesize a physical structure that realizes a given inductance matrix while finding an optimal tradeoff between volume and efficiency. This question arises often in power electronics, particularly in the context of components such as transformers and integrated magnetics [3], [4]. It also arises in the creation of coreless magnetics for parasitic compensation in filters [5]. In some cases the problem has been extended to include both inductive and capacitive reactances as part of the synthesis [6], [7]. This includes L-C-T structures which are designed to provide isolation and specific impedance characteristics, such as a series resonance to replace the tank and transformer in a resonant converter [8], [9]. Such integrated designs usually employ magnetic materials. The resulting constrained flux path provides for simplifying assumptions that lead to analytical design equations which make finding an optimal structure relatively straightforward.

In the case of VHF switching frequencies, air-core magnetics are the norm because this avoids prohibitive core losses. Without a well-defined flux path, finding an analytical solution to the inductance and resistance for most geometries is extremely difficult. For the planar transformer structures considered here (see Figure 1), previous work provides analytical solutions for the mutual and self inductances [10], but not the self or mutual ac resistance [11], nor a means to compensate for the change in inductance that arises when two coils are brought into close proximity. In the work by Tang [12] expressions are proposed to estimate efficiency, but these are accomplished by curve-fitting to experimental

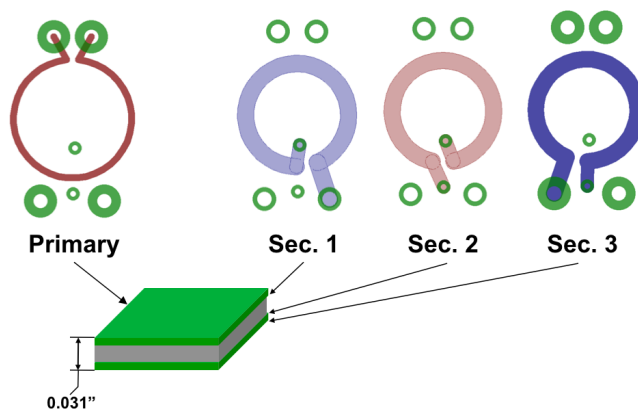


Fig. 1. A 4-layer transformer with a 1-turn primary and 3-turn secondary. Each turn is on a separate layer which avoids increased loss due to flux shielding as compared to spiral designs.

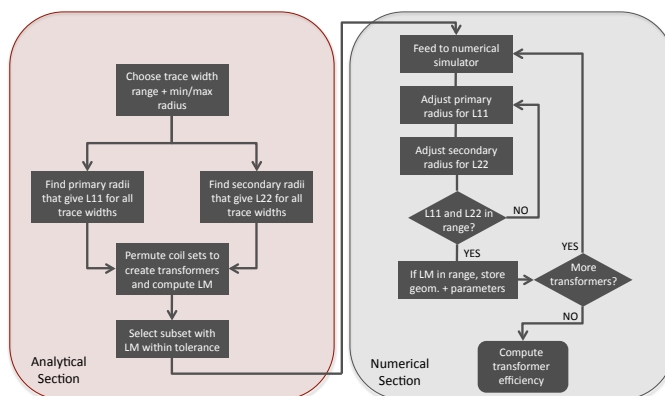


Fig. 2. Transformer synthesis algorithm

measurements and are only valid for a very specific set of structures and parameter variations.

In this work, the transformer magnetizing and leakage inductances serve as an integral part of the converter energy storage. This is desirable at VHF because it circumvents the need to design around transformer parasitics and it reduces the component count of the power stage, aiding the ultimate goal of achieving a tightly co-packaged system. With the leakage and magnetizing inductances playing a critical role in tuning the converter to operate efficiently at VHF, the transformer's inductance matrix is fully specified by the converter tuning point. Designing a transformer with the right inductance parameters and a good trade-off between volume and efficiency thus requires the ability to accurately compute the inductances and ac resistances at the operating frequency of the structure while including skin and proximity effects. This is possible for a given structure using any number of finite element field-solver packages.

While numerical solution can provide the accuracy required, it comes at the penalty of a heavy computational burden. For the relatively simple geometry of a two-winding planar transformer, simulation of a single design at sufficient accuracy for our purposes can be accomplished in a matter of a few minutes. However, answering the inverse problem with numerical simulation—finding which geometry provides the desired inductances and satisfies size and efficiency constraints—requires many successive simulations. The algorithm takes the form of evaluating a large pool of candidate geometries, picking those that match the inductance matrix, and analyzing the efficiency of the matching subset to find the loss-size tradeoff. If the pool of potential candidates is too large the computational overhead is massive, too small and a good design may never materialize. Thus the effort in solving this synthesis problem is establishing a means of finding acceptable designs without requiring more computation than may be performed in a reasonable amount of time.

The method applied here is illustrated in Figure 2. It breaks the process into two subsections. The first portion uses analytical expressions for the self and mutual inductance (e.g. those in [10]) to rapidly find a locus of geometries with the right inductance matrix. This greatly reduces the number of cases that need numerical evaluation and thus the total simulation time. The process begins with the selection of a desired range of trace widths for each of the primary and secondary coils.<sup>1</sup> For each trace width, a bisection algorithm finds the radius that gives the correct self inductance,  $L_{11}$  for the primary and  $L_{22}$  for the secondary. The bisection algorithm starts by computing the inductance at the minimum and maximum permitted radii, and a radius midway between them. Of the two ranges created, the range bounding the solution is selected and then halved again. The process is repeated until the range converges to within a predetermined tolerance of the desired inductance. The two sets of coils are then permuted into transformers by pairing each primary coil with each secondary coil. The mutual inductance for each coil pair is then calculated. All transformer geometries with mutual inductances within a predetermined range of the desired value (in this case approximately 20%) are saved and submitted for numerical analysis.

Numerical analysis is necessary for two reasons: it permits the calculation of the ac resistances and it accounts for proximity effects that are completely ignored by the analytical formulations. For each geometry computed analytically, the numerical section begins by computing the self inductance of the primary coil, with the secondary coil included in the analysis. The radius of the primary coil is then adjusted using a bisection algorithm until the desired  $L_{11}$  is achieved. This usually only requires a few tries. Once  $L_{11}$  is established, the process is repeated on the secondary. The secondary radius is changed, via bisection, until the value of  $L_{22}$  is achieved to within the preset tolerance of the desired value. At this point the value of  $L_{11}$  is re-checked to ensure that the changes to

<sup>1</sup>When the coil consists of multiple turns, the trace width and radius is identical for each turn. This limits the total number of geometries that need to be analyzed to a size that can be handled quickly on a typical computing resource. Only a very small gain in efficiency was realized by optimizing over the full set of parameters.

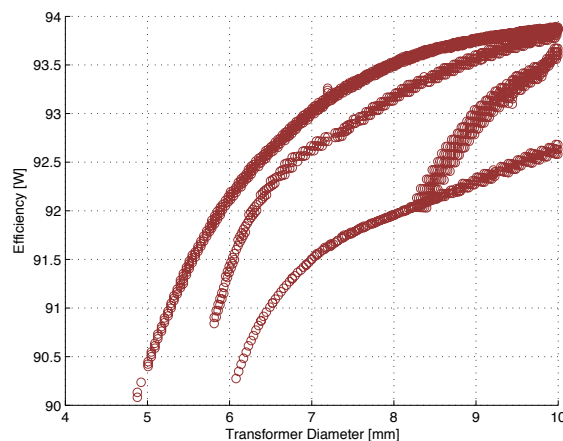


Fig. 3. Efficiency of 4-layer transformers for 10-Watt secondary power. The top left set of points is for 1-turn primary, 3-turn secondary.

the secondary have not pushed the value out of range. If it is out of range, bisection of  $L_{11}$  begins again, this time with the last radius of  $L_{22}$  as determined by the numerical simulator. Next the secondary is adjusted and the values of  $L_{11}$  and  $L_{22}$  rechecked. The process is repeated until both are within range. For a small number of cases, a limit cycle is reached whereby adjustment of the primary throws the secondary out of range and adjustment of the secondary does the same to the primary. This is dealt with by first reducing the step size by which the radius is changed. If it still fails to converge, an iteration limit is eventually reached and the coil pair is rejected.

Once the primary and secondary coils have the correct self inductances while in proximity, the mutual inductance is checked.<sup>2</sup> Coil pairs that have mutual inductances within the desired range of  $L_M$  are saved. This final set of cases represents the transformers that will provide the full desired inductance matrix. These are evaluated for efficiency by using the time-domain waveforms of the converter simulation from which the original inductance parameters were derived. The output is a plot such as that of Figure 3, which provides the efficiency-volume tradeoff for the choice of substrate and geometry in the context of the converter design. Final selection is a matter of the relative importance of volume versus efficiency.

### III. EXPERIMENTAL RESULTS

#### A. Transformers

An isolated  $\Phi_2$  converter was designed (the details will be included in the full paper) using the techniques outlined in [1] giving target inductance values for the transformer of  $L_{11} = 11.8$  nH,  $L_M = 11.8$  nH, and  $L_{22} = 47$  nH, which corresponds to a coupling coefficient of about 0.5. Simulations using a combination of MATLAB for analytical calculation and simulation control and FastHenry and Comsol as the field solvers were performed for two distinct sets of transformers: 2-layer spiral windings and 4-layer, 1-turn-per-layer windings.

<sup>2</sup>The mutual inductance is actually calculated during the evaluation of the self inductances, but it is not utilized until they are brought within tolerance.

TABLE I  
4-LAYER TRANSFORMER WINDING CONFIGURATIONS

Layer (z-location)	1T-3T	1T-2T	1T-2T (sub)
1 (0)	P	P	N/A
2 (7.2 mil)	S	S	P
3 (21.9 mil)	S	S	S
4 (31 mil)	S	N/A	S

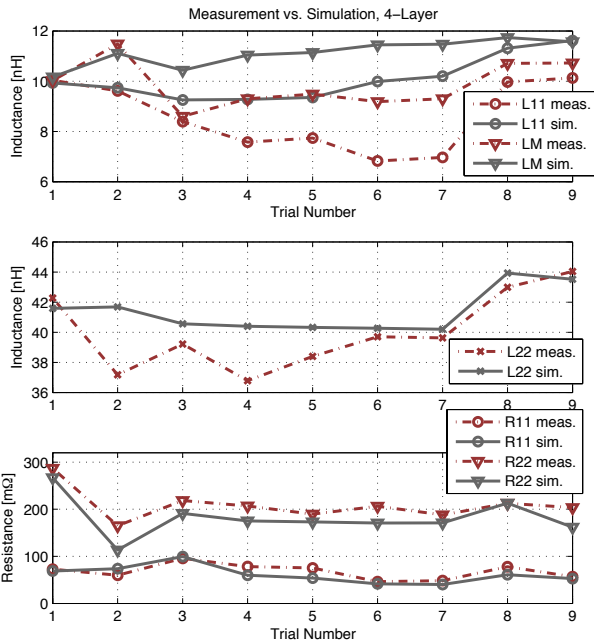


Fig. 4. Comparison of simulated and measured transformer parameters for 4-layer substrate

In the case of the 4-layer designs multiple winding configurations were checked. The three most successful are outlined in Table I. For each winding configuration multiple PCB substrates were simulated ranging in finished thickness from 20 mils to 62 mils. The 31-mil substrate provided the overall best performance. Figure 3 shows a scatter plot of successful transformer designs on a 31-mil, 4-layer substrate. The best loss-volume trade-off is achieved for a 1-turn primary and 3-turn secondary, corresponding to the top left set of points.

Two sets of transformers corresponding to a subset of the simulated designs were fabricated, the first on a 2-layer, 31-mil substrate had planar spiral windings. The second set fabricated, having 1-turn-per-layer windings, was on a 4-layer, 31-mil, substrate. In this case the transformers had up to 4-turns total (primary + secondary) with all of the winding configurations from Table I. Both sets of transformers were measured on an Agilent 4195a impedance analyzer to extract the inductance and resistance parameters.

The 2-layer agreement between measurement and simulation is relatively poor, with  $R_{11}$ , the primary winding ac resistance, being as much as four times higher than the simulated values. The error in mutual inductance, the largest deviation for the inductance parameters, was up to 42%. In

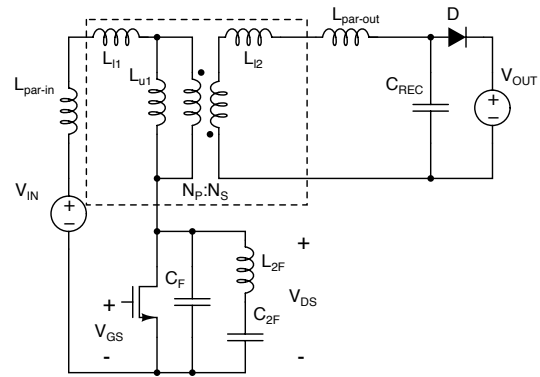


Fig. 5. 75 MHz, Isolated  $\Phi_2$  converter,  $L_{L1}=6.5\text{nH}$ ,  $L_{L2}=11.5\text{nH}$ ,  $L_{\mu 1}=3.6\text{nH}$ ,  $N_P=1$ ,  $N_S=3$ ,  $L_{2F}=15\text{n}$ ,  $C_{2F}=75\text{p}$ ,  $C_{REC}=10\text{p}$ ,  $L_{par-in}=2.2\text{nH}$ ,  $L_{par-out}=1\text{nH}$ , Diode: 2 x ON SS-16, Mosfet: Custom BCD,  $V_{IN}=8\text{-}16\text{V}$ ,  $V_{OUT}=12\text{V}$ .

particular, the errors are largest for designs that have multi-turn primary windings which cause excessive flux shielding. This is not well captured by the numerical simulator leading to designs with too much copper in the center of the winding. This results in much higher resistance and lower inductance than predicted by simulation.

The data from the 4-layer set (Figure 8) shows better agreement, particularly in the case of resistance which shows a maximum error of about 35%. The maximum inductance error was about 37%. The 4-layer, single-turn-per-layer, designs such as those of Figure 1, avoid the flux shielding issues of the 2-layer designs. This not only improves agreement between simulation and experiment, but it results in much lower ac resistance. This, in turn, corresponds to much better efficiency.

## B. Converter

A transformer from the 4-layer fabrication run was selected to demonstrate operation in a VHF dc-dc converter. The topology is an isolated  $\Phi_2$  converter with a switching frequency of 75 MHz. Figure 5 shows the converter schematic with the transformer highlighted with dotted lines, as well as parasitic inductances  $L_{par-in}$  and  $L_{par-out}$  in the input and output loops respectively. The original design was accomplished before transformer synthesis was undertaken.

The transformer parameters are  $L_M=10.83\text{ nH}$ ,  $L_{11}=10.1\text{ nH}$ ,  $L_{22}=44\text{ nH}$ ,  $R_{11}=57\text{ m}\Omega$ ,  $R_{22}=204\text{ m}\Omega$ , and max outer diameter of 7.8 mm. The inductances differ from the desired values by as much as 14.4%. Since the transformer energy storage is an integral part of the  $\Phi_2$  resonant network, the network design had to be compensated to get proper operation. This was possible by adjusting the capacitances  $C_F$  and  $C_{REC}$  and the characteristic impedance of the 2nd harmonic resonator formed by  $C_{2F}$  and  $L_{2F}$  to find a different tuning point that satisfies zero-voltage-switching operation. The final component values are detailed in the caption of Figure 5.

An additional consideration that affected the final tuning point of the converter is the input loop parasitic inductance,  $L_{par-in}$ . At 3 nH it acts as an impedance divider, reducing the drive signal at transformer primary without a matching reduction in circulating currents. This has the effect of driving

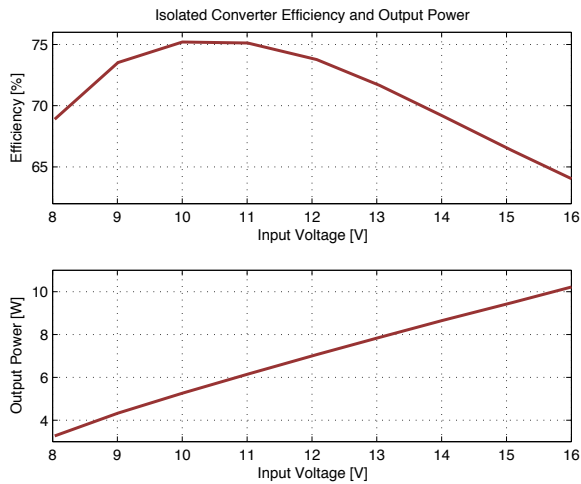


Fig. 6. Experimental power and efficiency for the isolated  $\Phi_2$  converter.

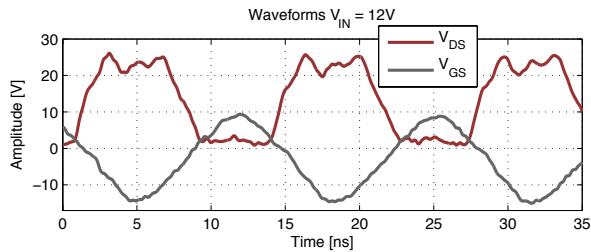


Fig. 7. Measured waveforms for the isolated  $\Phi_2$  converter.

down efficiency and output power. However, since this inductance appears in series with the primary leakage,  $L_{l1}$ , it can be compensated by reducing  $L_{l1}$  in a second iteration of the transformer design.

Figure 6 shows the experimental output power and efficiency of the converter. At the nominal operating point of

TABLE II  
CONVERTER LOSS BREAKDOWN

Loss	Value ( $V_{IN}=12$ V)
Switch	928 mW
Diode	379 mW
$L_{2F}$	85 mW
Transformer	620 mW

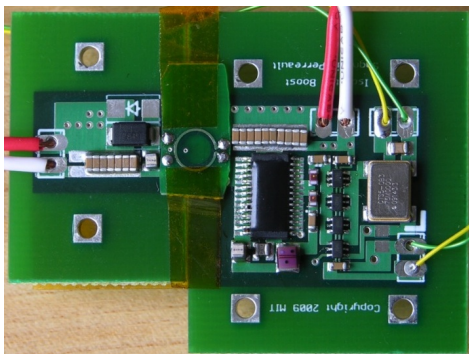


Fig. 8. Prototype Isolated  $\Phi_2$  Converter

$V_{IN} = 12$  V, the power is about 7 W and drain efficiency 74%. The estimated transformer loss is listed in Table II, the loss breakdown for the converter operating at the nominal  $V_{IN}$ . This corresponds to a transformer efficiency of 91% in the converter. Finally, the converter drain and gate voltage waveforms (Figure 7) show the desired characteristics of the resonant  $\Phi_2$  power stage including near ZVS operation.

#### IV. CONCLUSION

The synthesis of air-core magnetic components to realize a specified inductance matrix is feasible with current numerical simulation techniques. For the planar transformer design demonstrated here, an augmented grid search can reach a solution in less than 48 hours when run as a single thread. The nature of the search algorithm allows it to be readily parallelized, and solution times an order of magnitude shorter have been achieved. The maximum transformer parameter deviations are small enough to permit reasonable converter operation with minimal retuning. An experimental transformer 7.8 mm in diameter is able to transfer 7 watts at 91% efficiency in an isolated  $\Phi_2$  converter operating at 75 MHz with an overall power-stage efficiency of 74%.

#### REFERENCES

- [1] J. M. Rivas, Y. Han, O. Leitermann, A. D. Sagneri, and D. J. Perreault, "A high-frequency resonant inverter topology with low-voltage stress," *IEEE Transactions on Power Electronics*, vol. 23, pp. 1759–1771, July 2008.
- [2] R. C. N. Pilawa-Podgurski, A. D. Sagneri, J. M. Rivas, D. I. Anderson, and D. J. Perreault, "Very-high-frequency resonant boost converters," *IEEE Transactions on Power Electronics*, vol. 24, pp. 1654–1665, 2009.
- [3] G. W. Ludwig and S.-A. El-Hamamsy, "Coupled inductance and reluctance models of magnetic components," *IEEE Transactions on Power Electronics*, vol. Vol. 6, pp. pp. 240–250, April 1991.
- [4] R. P. Severns and G. E. Bloom, *Modern DC-DC Switchmode Power Converter Circuits*. Bloom Associates, Inc., 1985.
- [5] T. C. Neugebauer and D. J. Perreault, "Filters with inductance cancellation using printed circuit board transformers," *IEEE Transactions on Power Electronics*, vol. vo. 19, no. 3, pp. pp 591–602, May 2004.
- [6] J. Phinney, J. Lang, and D. Perreault, "Multi-resonant microfabricated inductors and transformers," in *Power Electronics Specialists Conference, 2004. PESC 04. 2004 IEEE 35th Annual*, vol. 6, pp. 4527–4536, 20-25 June 2004.
- [7] M. Ehsani, O. H. Stielau, J. D. van Wyk, and I. J. Pitel, "Integrated reactive components in power electronic circuits," *IEEE Transactions on Power Electronics*, vol. vol. 8, pp. pp. 208–215, 1993.
- [8] I. W. Hofsjager, J. Ferreira, and J. van Wyk, "Optimised planar integrated l-c-t components," in *Power Electronics Specialists Conference, 1997.*, vol. vol. 2, pp. pp. 1157–1163, June 1997.
- [9] K. Lai-Dac, Y. Lembeye, A. Besri, and J.-P. Keradec, "Analytical modeling of losses for high frequency planar lct components," in *The 2009 IEEE Energy Conversion Congress and Exposition (ECCE), San Jose*, September 2009.
- [10] W. G. Hurley and M. C. Duffy, "Calculation of self and mutual impedances in planar magnetic structures," *IEEE Transactions on Magnetics*, vol. Vol. 31, No. 4, pp. 2416–2422, 1995.
- [11] J. H. Spreen, "Electrical terminal representation of conductor loss in transformers," *IEEE Transactions on Power Electronics*, vol. vol. 15, no. 4, no. no. 4, pp. pp. 424–429, Oct. 1990.
- [12] S. C. Tang, S. Y. Hui, and H. S.-H. Chung, "Coreless planar printed-circuit-board (pcb) transformers- a fundamental concept for signal and energy transfer," *IEEE Transactions on Power Electronics*, vol. Vol. 15, pp. pp. 931–941, Sept. 2000.